Received 29 August 2022, accepted 24 September 2022, date of publication 30 September 2022, date of current version 10 October 2022.

Digital Object Identifier 10.1109/ACCESS.2022.3210968

RESEARCH ARTICLE

Active Vibration Control of Railway Vehicle Car Body by Secondary Suspension Actuators and Piezoelectric Actuators

HUI CAO[1], GANGJUN LI[1], AND NING LIANG[2]
[1]College of Intelligent Manufacturing, Chengdu Technological University, Chengdu 611730, China
[2]Sichuan Technology and Business College, Chengdu 611830, China

Corresponding author: Hui Cao (ch_hello@163.com)

This work was supported by the Doctoral Fund of Chengdu Technological University under Grant 2019RC011.

ABSTRACT Active vibration suppression of high-speed electric multiple unit (EMU) car bodies was studied by the combined use of secondary suspension actuators and piezoelectric actuators. A vertical dynamics model was established considering secondary suspension actuators and piezoelectric actuators. The positions of the piezoelectric actuators and sensors were optimized using H_2 and H_∞ norms. The feedback controller was designed using a robust optimal control method. The effects of the vibration devices and active control methods on the vehicle dynamic performance were simulated using MATLAB. The dynamic performance differences among the passive suspension vehicle, secondary vertical actuator installation vehicle, and active vibration control vehicle were compared and analyzed. The results show that the piezoelectric actuators and piezoelectric sensors were arranged at distances of 7.15, 12.25, and 17.35 meters from the left end of the car body, and the normalized H_2 and H_∞ norms of the first and second order elastic modes of the car body were the largest, which can be used as piezoelectric actuators and sensor placement positions. Secondary suspension actuators can reduce rigid car body vibrations, and piezoelectric actuators can reduce elastic vibration. The higher the speed, the better is the acceleration suspension effect. When the vehicle speeds were 200 km$\cdot$h^{-1} and 350 km$\cdot$h^{-1}, the vehicle vibration acceleration decreased by 10% and 18%, respectively. Compared with the passive suspension system, the active vibration suspension system with a robust controller can reduce the rigid and elastic vibrations of the vehicle and improve ride comfort.

INDEX TERMS EMU car body, piezoelectric actuator, secondary suspension actuator, robust control, vibration control.

I. INTRODUCTION

The maximum operating speed is a comprehensive indicator of the technical level of high-speed railway vehicles. In the process of car body design, aluminum alloy is used instead of stainless steel and a sandwich structure is used instead of a solid structure. This makes the vehicle lighter and makes it easier to achieve higher speeds, which addresses cost-effectiveness and energy efficiency. However, lightweight design leads to more flexibility and lower modal frequency, and the exogenous disturbances can excite the structural vibration more easily. At the same time, with increasing vehicle speed, the track excitation frequency is increased, and the wheel-rail contact force is changed, which could cause serious elastic vibration. This vibration frequency is in the sensitive frequency range of the human body, thus affecting the passenger ride comfort. Vibration causes vehicle structure fatigue, affecting the dynamic performance and service life [1], [2], [3]. Therefore, the suppression of vibration of flexible modes as well as rigid modes of vehicle structures is important in order to provide appropriate dynamic performance and passenger ride quality.

Many researchers have attempted to suppress the vibration of car bodies. Huang *et al.* attached a damping elastic material

The associate editor coordinating the review of this manuscript and approving it for publication was Zhigang Liu.

to the vehicle body, reduced the elastic vibration of the vehicle body, and improved ride comfort by increasing the damping of the vehicle body [4]. Schandl *et al.* installed a piezoelectric actuator in an appropriate part of the underframe of a subway vehicle body and adopted a robust feedback control method to control the vibration of the vehicle body. The effectiveness of the method was verified through simulations and model tests [5]. Foo *et al.* installed an electro-hydraulic actuator in the secondary suspension of a car body, installed an electromagnetic actuator in the middle of the car body, and adopted the skyhook damping control theory to reduce the elastic vibration caused by the lightweight design of the car body [6]. Sugahara *et al.* installed damping control devices in primary and secondary suspensions to reduce car body vibration, and the results of both simulations and vehicle running tests demonstrated that this system reduced vertical vibrations in the bogies and the car body using the sky-hook control theory [7].

Because the first vertical bending mode has the greatest contribution to the elastic vibration of the vehicle car body [3], [8], the damping control devices installed on the air spring are placed near the node of the first vertical bending mode of the vehicle car body, which affects the rigid vibration of the car body, and the elastic vibration is not suppressed effectively. With the improvement of the manufacturing process of piezoelectric intelligent structures, the output force can meet the requirements of the working force in large-structure elastic vibration control. The piezoelectric intelligent structure has the advantages of being lightweight and having a low energy consumption. It has a positive effect on the vibration of a flexible structure [9], [10].

The positions of the piezoelectric actuators and sensors are important for the efficient control of flexible structures. Many optimization criteria have been proposed for the position optimization of piezoelectric elements. The criterion proposed by Leleu *et al.* was based on system observability and controllability [11]. The criterion of Gawronski is based on H_2, H_∞, or the Hankel system norm of the transfer function matrices from the actuators to the sensors [12]. Benatzky and Kozek investigated the influence of actuator size on the closed-loop stability of collocated and non-collocated transfer function models utilized in the structural control of flexible beams [13].

The purpose of this paper is to propose a new method of suppressing both the vertical rigid mode vibration and vertical flexible mode vibration of a car body by using a robust optimal control method for secondary suspension actuators and piezoelectric actuators. The secondary suspension actuators suppress the lower frequency vibration of rigid motion, while the piezoelectric actuators introduce a damping force to suppress the flexible vibration. A robust optimal control strategy based on the combined use of piezoelectric and secondary suspension actuators was investigated. The results showed that the vertical vibrations of the car body were completely suppressed, and the ride quality was improved.

II. VEHICLE MECHANICS MODEL

A vehicle model considering the vibration reduction device shown in Fig. 1 was established to analyze the vibration control effect of the vibration reduction device on the vehicle. It includes the car body, bogie frames, wheelsets, suspensions, and actuators. Electrohydraulic actuators were installed in the secondary suspension, and piezoelectric actuators were mounted on the side frame of the car body underframe. The car body is considered to be an elastic homogeneous Euler-Bernoulli beam. Origin O of the coordinate system is located at the left end of the car body. The bogie and wheelsets were considered rigid bodies. It is assumed that no wheel jump occurs, and the vertical movements of the wheelsets are the same as the track irregularities. In Fig. 1, v is the train speed, L is the car body length, L_s is the half of the distance between the centers of bogies, m_c is the mass of car body, I_c is the pitch inertia of the car body, m_b is the mass of bogie, I_b is the pitch inertia of the bogie, c_1 and c_2 are the primary and secondary damping coefficients respectively, k_1 and k_2 are the primary and secondary spring stiffness respectively, U_1 and U_2 are the control forces of the right and left secondary suspension actuators respectively, b It is the half of the wheelbase of the bogies, $z(x, t)$ is the vertical vibration displacement of the car body, including the displacement of the rigid body and elastic body, x is the coordinate of the longitudinal position of the car body, t is the running time of the vehicle, θ_c is the pitch displacement of the car body, z_c is the displacement of the car body, z_{b1} and z_{b2} are the bounce displacements of the bogie respectively, θ_{b1} and θ_{b2} are the right and left bogie frame pitch displacements respectively, $z_{w1} \sim z_{w4}$ are the vertical displacements of first to fourth wheelsets. According to the vibration theory of the beam, the car body partial differential equation can be obtained as follows [14]:

$$EI\frac{\partial^4 z(x,t)}{\partial x^4}+\rho A\frac{\partial^2 z(x,t)}{\partial t^2}+\phi I\frac{\partial^5 z(x,t)}{\partial x^4 \partial t} = \sum_{i=1}^{2} F_i\delta(x-x_i)+\sum_{l=1}^{n} M_l(x,t)[\dot{\delta}(x-x_{l2})-\dot{\delta}(x-x_{l1})] \tag{1}$$

where EI, ρA, and ϕI denote the bending stiffness, mass per unit length, and internal damping coefficient of the beam, respectively; x_i is the longitudinal position coordinate of the secondary suspension of the car body; F_i is the force acting on the bogie secondary suspension; $\delta(x)$ is the Dirac delta function; n is the number of piezoelectric actuators; x_{l1}, x_{l2} are the coordinates of the two fixed ends of the lth piezoelectric actuator; and $M_l(x, t)$ is the torque acting on the car body by the lth piezoelectric actuator acting on the vehicle body, which can be expressed as [15]

$$M_l(x,t) = RV_l H[x(x-x_{l1}) - x(x-x_{l2})]$$
$$R = dgE_p z_p \tag{2}$$

where R is the piezoelectric actuator torque coefficient, V_l is the voltage applied to the lth actuator, $H(*)$ is the Heaviside function, d is the piezoelectric strain coefficient, g is the width of the piezoelectric actuator, E_p is the actuator elastic modulus, and z_p is the height of the piezoelectric actuator relative to the neutral axis of the car body.

According to normal Newtonian mechanics, there is

$$F_i = -c_2[\dot{z}(x_i,t) - \dot{z}_{bi}] - k_2[z(x_i,t) - z_{bi}] + U_i \tag{3}$$

where U_i is the control force from the secondary suspension actuators.

Because the car body is regarded as a uniform Euler beam, the bounce vibration eigenfunction is considered as $Y_1(x) = 1$, and the pitch vibration eigenfunction is considered as $Y_2(x) = x - L/2$. Because the stiffness and damping of the second suspension of the car body are small, it can be regarded as a free Euler beam, and the rth modal function of the elastic vibration is.

$$\begin{aligned} Y_r(x) &= \mathrm{ch}(\beta_r x) + \cos(\beta_r x) - \frac{\mathrm{ch}(\beta_r L) + \cos(\beta_r L)}{\mathrm{sh}(\beta_r L) + \sin(\beta_r L)} \\ &\quad \cdot [\mathrm{sh}(\beta_r x) + \sin(\beta_r x)] \\ \beta_r &= \frac{(2r+1)\pi}{2L} \end{aligned} \tag{4}$$

where β_r is the variable related to the car body structure parameters and frequency.

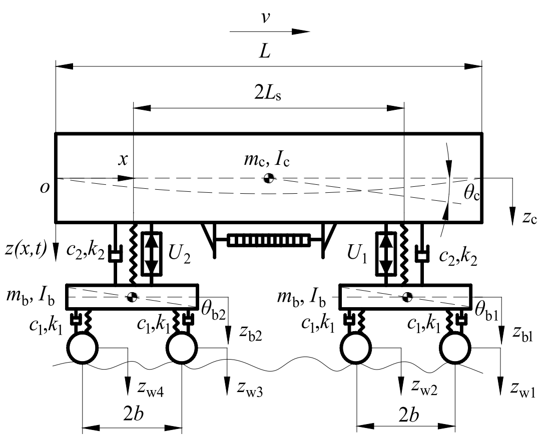

FIGURE 1. Vehicle mechanics model of vibration reduction.

It was assumed that $q_r(t)$ denotes the principal coordinates of the rth mode. Considering *the* N modes of the car body, the vibration displacement can be written as

$$z(x,t) = z_c + (x - L/2)\theta_c + \sum_{r=3}^{N} Y_r(x) q_r(t) \tag{5}$$

By substituting equation (5) into equation (1) and integrating along the length of the car body, considering the orthogonality of the eigenfunction and the characteristic of the delta function, the vibration equations of the car body and bogie are

$$\begin{cases} \ddot{q}_r(t) + 2\xi_r\omega_r\dot{q}_r(t) + \omega_r^2 q_r(t) \\ = \dfrac{1}{m_c}\displaystyle\sum_{i=1}^{2} Y_r(x_i)F_i \\ \qquad + \dfrac{R\sum_{l=1}^{n}[\dot{Y}_r(x_{l2}) - \dot{Y}_r(x_{l1})]V_l}{m_c} \\ m_c\ddot{z}_c = \displaystyle\sum_{i=1}^{2} F_i \\ I_c\ddot{\theta}_c = \displaystyle\sum_{i=1}^{2} F_i(x_i - L/2) \\ m_b\ddot{z}_{b1} + c_2[\dot{z}_{b1} - \dot{z}(x_1,t)] + k_2[z_{b1} - z(x_1,t)] + c_1(2\dot{z}_{b1} \\ \qquad - \dot{z}_{w1} - \dot{z}_{w2}) + k_1(2z_{b1} - z_{w1} - z_{w2}) = -U_1 \\ m_b\ddot{z}_{b2} + c_2[\dot{z}_{b2} - \dot{z}(x_2,t)] + k_2[z_{b2} - z(x_2,t)] + c_1(2\dot{z}_{b2} \\ \qquad - \dot{z}_{w3} - \dot{z}_{w4}) + k_1(2z_{b2} - z_{w3} - z_{w4}) = -U_2 \\ I_b\ddot{\theta}_{b1} + c_1 b(2b\dot{\theta}_{b1} - \dot{z}_{w1} + \dot{z}_{w2}) + k_1 b(2b\theta_{b1} \\ \qquad - z_{w1} + z_{w2}) = 0 \\ I_b\ddot{\theta}_{b2} + c_1 b(2b\dot{\theta}_{b2} - \dot{z}_{w3} + \dot{z}_{w4}) + k_1 b(2b\theta_{b2} \\ \qquad - z_{w3} + z_{w4}) = 0 \end{cases}$$

$$\begin{aligned} \omega_r^2 &= \frac{EI\beta_r^4}{\rho A} \\ 2\xi_r\omega_r &= \frac{\phi I\beta_r^4}{\rho A} \end{aligned} \tag{6}$$

where ξ_r and ω_r denote the damping ratio and angular frequency, respectively, of the rth-order bending mode of the car body.

Setting the displacement vector is

$$\mathbf{z} = (z_c, \theta_c, z_{b1}, z_{b2}, \theta_{b1}, \theta_{b2}, q_3(t), \ldots, q_N(t))^{\mathrm{T}} \tag{7}$$

The system vibration differential equation can be written as

$$\begin{aligned} &\mathbf{M\ddot{z}} + \mathbf{C\dot{z}} + \mathbf{Kz} \\ &\quad = \mathbf{F} + \mathbf{D}_1\mathbf{U} + \mathbf{D}_2\mathbf{Z}_1 \\ &\mathbf{F} = \begin{bmatrix} 0 \\ R\sum_{l=1}^{n}[\dot{Y}_r(x_{l2}) - \dot{Y}_r(x_{l1})]V_l \end{bmatrix} \\ &\mathbf{D}_1 = \begin{bmatrix} -1 & L_s & 1 & 0 & 0 & 0 & Y_3(x_1) & \cdots & Y_N(x_1) \\ -1 & -L_s & 0 & 1 & 0 & 0 & Y_3(x_2) & \cdots & Y_N(x_2) \end{bmatrix}^{\mathrm{T}} \\ &\mathbf{D}_2 = \begin{bmatrix} 0 & 0 & k_1 & 0 & k_1 b & 0 & 0 & 0 \\ 0 & 0 & c_1 & 0 & c_1 b & 0 & 0 & 0 \\ 0 & 0 & k_1 & 0 & -k_1 b & 0 & 0 & 0 \\ 0 & 0 & c_1 & 0 & -c_1 b & 0 & 0 & 0 \\ 0 & 0 & 0 & k_1 & 0 & k_1 b & 0 & 0 \\ 0 & 0 & 0 & c_1 & 0 & c_1 b & 0 & 0 \\ 0 & 0 & 0 & k_1 & 0 & -k_1 b & 0 & 0 \\ 0 & 0 & 0 & c_1 & 0 & -c_1 b & 0 & 0 \end{bmatrix}^{T} \\ &\mathbf{Z_1} = (z_{w1}, \dot{z}_{w1}, z_{w2}, \dot{z}_{w2}, z_{w3}, \dot{z}_{w3}, z_{w4}, \dot{z}_{w4})^{\mathrm{T}} \\ &\mathbf{U} = (U_1, U_2)^{\mathrm{T}} \end{aligned} \tag{8}$$

where $\mathbf{M}$, $\mathbf{K}$ and $\mathbf{C}$ are the vehicle system inertia, stiffness, and damping matrix, respectively; $\boldsymbol{F}$ is the piezoelectric actuator output force vector; $\mathbf{D}_1$ is the secondary suspension actuator coefficient matrix; $\mathbf{D}_2$ is the track irregularity input matrix; U_1 and U_2 are the secondary suspension actuator output forces; and $\mathbf{Z}_1$ is the track irregularity vector.

Let the state vector be

$$\mathbf{X} = (\mathbf{z}, \dot{\mathbf{z}})^{\mathrm{T}} \tag{9}$$

Equation (9) is written as

$$\begin{aligned}
\dot{\mathbf{X}} &= \mathbf{A}\mathbf{X} + \mathbf{B}_1\mathbf{Z}_1 + \mathbf{B}_2\mathbf{U} + \mathbf{B}_3\mathbf{V} \\
\mathbf{A} &= \begin{bmatrix} 0 & \mathbf{I} \\ -\mathbf{M}^{-1}\mathbf{K} & -\mathbf{M}^{-1}\mathbf{C} \end{bmatrix} \\
\mathbf{B}_1 &= \begin{bmatrix} \mathbf{0} \\ \mathbf{M}^{-1}\mathbf{D}_2 \end{bmatrix} \\
\mathbf{B}_2 &= \begin{bmatrix} 0 \\ \mathbf{M}^{-1}\mathbf{D}_1 \end{bmatrix} \\
\mathbf{B}_3 &= R[\dot{Y}_r(x_{l2}) - \dot{Y}_r(x_{l1})] \begin{bmatrix} 0 \\ \mathbf{M}^{-1} \end{bmatrix} \\
\mathbf{V} &= (V_1, V_2 \ldots, V_l, \ldots, V_n)^{\mathrm{T}}
\end{aligned} \tag{10}$$

III. ACTUATOR AND SENSOR POSITION ARRANGEMENT

Because of the narrow space of the secondary suspension of the car body, the choice of secondary vertical actuators is limited. Foo *et al.* showed that an electro-hydraulic servo actuator can be adopted, and the power and frequency response can meet these requirements [6]. The piezoelectric actuators and sensor mounting positions have a significant influence on the vibration damping effect of the car body. The control forces and signals originate from the piezoelectric actuators and sensors. If they are installed at elastic vibration nodes, no force or sensing signals are generated. Therefore, the H_2 and H_∞ criteria can be used to optimize piezoelectric actuator arrangement [16]. To achieve collocation control of the piezoelectric actuator, piezoelectric actuators and piezoelectric sensors were placed on both sides of the same portion. Owing to the greater force required to reduce the vibration of the car body, piezoelectric actuators adopt the piezoelectric stack working mode to meet these requirements.

For the vehicle control system shown in Fig. 1, the piezoelectric actuator control voltages are the input, the vertical vibration displacement of the car body is the output, and the H_2 and H_∞ norms of the system transfer function are

$$\begin{cases} \|G(s)\|_2 = \dfrac{1}{2\pi}\displaystyle\int_{-\infty}^{+\infty} \operatorname{trace}\left[G^*(\mathrm{j}\omega)G(\mathrm{j}\omega)\right]\mathrm{d}\omega \\ \|G(s)\|_\infty = \sup\limits_{0\le\omega} \sigma_{\max}\left[G(\mathrm{j}\omega)\right] \end{cases} \tag{11}$$

where s is a complex variable, ω is the imaginary part of s, $G^*(\mathrm{j}\omega)$ is the complex conjugate of $G(\mathrm{j}\omega)$, and $\sigma_{\max}\left[G(\mathrm{j}\omega)\right]$ is the largest singular value of $G(\mathrm{j}\omega)$.

The H_2 norm represents the impulse response energy of the $G(s)$ system, and the minimum H_2 norm represents the minimum vibration energy of the system.

TABLE 1. Parameters of high-speed vehicle.

m_c /t	26
I_c/(t·m^2)	1 300
ρ/(t·m^{-3})	2.7
A/m^2	0.396
E / (kN·m^{-2})	6.9×10^6
I/m^4	0.52
m_b /t	2.44
I_b /(t·m^2)	1.4
c_1 / (kN·s·m^{-1})	30
c_2 / (kN·s·m^{-1})	50
k_1 / (kN·m^{-1})	2 400
k_2 / (kN·m^{-1})	380
L /m	24.5
L_S /m	8.75
b /m	1.25

Using the parameters of the EMU in Table 1, the first two elastic modes of the car body were considered. The normalized H_2 and H_∞ norms are shown in Fig. 2 and 3, respectively. It can be seen from Fig. 2 and Fig. 3 that the normalized H_2/H_∞ norm of the first and second car body elastic modes is the largest at 7.15, 12.25, and 17.35 m respectively, and can be used as arrangement position of piezoelectric actuators and sensors.

IV. CAR BODY VIBRATION REDUCTION METHOD

To achieve car body vibration control and meet the system robust control requirement, the H_∞ optimal control method

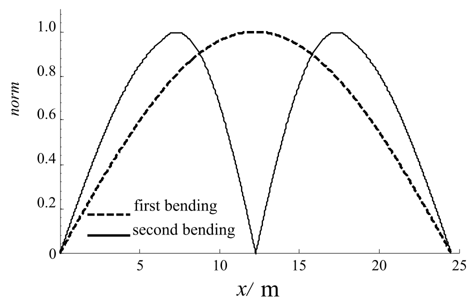

FIGURE 2. H_2 **norm of dimension 1.**

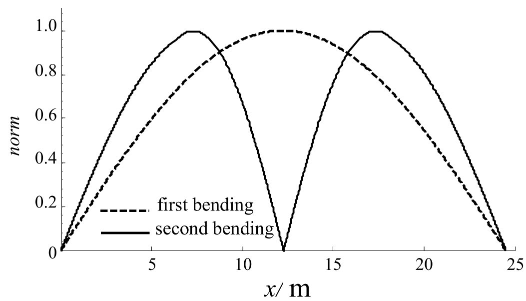

FIGURE 3. H_∞ **norm of dimension 1.**

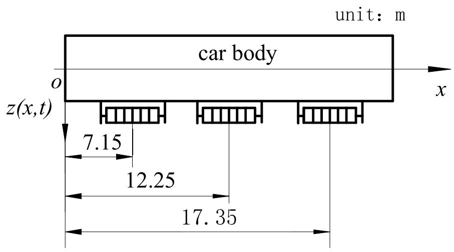

FIGURE 4. Piezoelectric actuator placement.

can be used [17], [18]. The basic idea of H_∞ control is that the influence of interference on the system is the smallest when the H_∞ norm of the system interference and the error transfer function is minimal. Therefore, the H_∞ norm can be used as a tool to optimize design.

The car body considers the rigid mode and the first two elastic modes; the bogie and wheelsets are regarded as rigid. The piezoelectric actuators were arranged as shown in Fig. 4. The state space of the system can be expressed as

$$\begin{aligned}
\dot{\mathbf{X}} &= \mathbf{AX} + \mathbf{B}_4\mathbf{w} + \mathbf{B}_5\mathbf{u} \\
\mathbf{Z}_2 &= \mathbf{C}_1\mathbf{X} + \mathbf{D}_{11}\mathbf{w} + \mathbf{D}_{12}\mathbf{u} \\
\mathbf{Y} &= \mathbf{C}_2\mathbf{X} + \mathbf{D}_{21}\mathbf{w} + \mathbf{D}_{22}\mathbf{u} \\
\mathbf{u} &= (U_1, U_2, V_1, V_2, V_3)^{\mathrm{T}} \\
\mathbf{D}_3 &= \begin{bmatrix} \mathbf{D}_{11} & \mathbf{D}_{12} \\ \mathbf{D}_{21} & \mathbf{D}_{22} \end{bmatrix} \\
\mathbf{B_4} &= \mathbf{B_1} = \begin{bmatrix} \mathbf{0} \\ \mathbf{M^{-1}D_2} \end{bmatrix} \\
\mathbf{B}_5 &= \begin{bmatrix} 0 & 0 \\ \mathbf{M}^{-1}\mathbf{D}_1 & K\left[\dot{Y}_r(x_{l2}) - \dot{Y}_r(x_{l1})\right]\mathbf{M}^{-1} \end{bmatrix}
\end{aligned} \tag{12}$$

where $\mathbf{w}$ is the external disturbance or excitation vector; $\mathbf{u}$ is the actuator control input vector; $\mathbf{Z}_2$ is the controlled variable vector, including the car body vertical acceleration, secondary vertical actuator control force, and piezoelectric actuator control voltage; $\mathbf{Y}$ is the measurement output vector, including the car body vertical vibration acceleration and secondary suspension deflection of the vehicle; A is the system matrix; B_4 is the disturbance input matrix; B_5 is the input matrix; C_1 is the performance output matrix; C_2 is the measurement output matrix; D_3 is the feed-through matrix; and V_1, V_2, V_3 is the piezoelectric actuator control voltage of the car body.

The measurement output is defined as

$$\mathbf{Y} = \begin{bmatrix} \ddot{z}_c \\ \ddot{\theta}_c \\ z_c - L_s\theta_c - z_{b1} + \sum_{r=3}^{N} Y_r(x)q_r(t) \\ z_c + L_s\theta_c - z_{b1} + \sum_{r=3}^{N} Y_r(x)q_r(t) \end{bmatrix} \tag{13}$$

That is, the output is the bounce acceleration, pitch acceleration of the car body, and deflection of the secondary suspension. The coefficient matrix is obtained from each vector.

A block diagram of the control system is shown in Fig. 5. The aims of this control are to reduce vertical vibration, improve ride comfort, and reduce the frequency response range of the controller. In Fig. 5, $K(s)$ is the controller transfer function, P is the nominal plant, W_Q is the weight function of measurement noise Q, $\mathbf{W_Y}$ is the weight function of measurement output Y, and $\mathbf{W_u}$ is the weight function of control input u. Therefore,

$$\begin{cases}
\mathbf{W_Y} = \mathrm{diag}(W_1, W_2) \\
\mathbf{W_u} = \mathrm{diag}(W_3, W_3, W_4, W_4, W_4) \\
W_1 = 50\dfrac{s^2 + 14s + 100}{s^2 + 6s + 100} \\
W_2 = 50 \\
W_3 = 0.001\dfrac{s^2 + 14s + 16}{s^2 + 14s + 100} \\
W_4 = 0.01\dfrac{s^2 + 8s + 100}{s^2 + 14s + 100}
\end{cases} \tag{14}$$

where W_1 denotes the vibration acceleration, W_2 denotes the deflection of the secondary suspension, W_3 denotes the vertical actuator of the secondary suspension, and W_4 denotes the weight function of the piezoelectric actuator.

V. SIMULATION RESULTS ANALYSIS

Using the parameters of the high-speed vehicle shown in Table 1, the parameters of the piezoelectric actuator shown in Table 2, and the robust control toolbox of MATLAB to program according to the H_∞ norm constrained method to design the state estimation optimal controller, the main steps are as follows.

Step 1: Establish a mathematical model, as expressed in equation (12), and clarify the controlled variables, measured variables, and disturbance inputs.

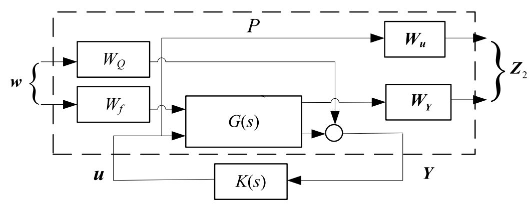

FIGURE 5. Structure of H_∞ control.

Step 2: According to the requirement, select the measurement noise, disturbance input, measurement output and control force weighting functions.

Step 3: Design the H_∞ feedback control law.

Step 4: Perform performance evaluation of the designed system by simulation. The evaluation indices are the vibration acceleration power spectral density (PSD) and acceleration root mean square (RMS) values. If the system satisfies the design requirements, the design is terminated. If not, return to Step 1 and redesign.

To analyze the vertical vibration reduction effect of the car body, it is necessary to analyze the self-vibration frequency and vibration mode of the car body. According to the method provided in [19], the vehicle parameters in Tab. 1 are used. The self-vibration frequencies and vibration modes are listed in Table 3.

The PSDs of the vibration acceleration in the middle of the car body and above the bogie were obtained by MATLAB simulation, and are shown in Fig. 6 and 7. It can be seen that the vibration acceleration PSDs below 18 Hz at the center of the car body and above the bogie are significantly reduced by the action of the vertical and piezoelectric actuators. At the first vertical bending vibration frequency, the PSDs in the middle of the car body decreased by 5% of the passive suspension, and the acceleration PSDs above the bogie decreased by 10% of the passive suspension. At the first vertical bending frequency of the car body, the effect of the secondary vertical actuators and piezoelectric actuators is significant compared to using only the secondary vertical actuator, which can significantly reduce the elastic vibration of the car body, indicating that the piezoelectric actuator has a significant effect on the first vertical elastic vibration of the car body.

TABLE 2. Parameter values of piezoelectric actuators.

Piezoelectric constant /(m•V^{-1})	6.8×10^{-10}
Length /m	0.194
Diameter of disk /m	0.045
Thickness of one disk /m	5×10^{-4}
Young's Modulus /(N•m^{-2})	6.4×10^{12}

TABLE 3. Analysis results of vehicle modes.

mode	frequency/Hz
bouncing of car body	0.83
pitching of car body	1.02
bounding of frame of bogie	7.33
pitching of frame of bogie	11.65
first vertical bending of car body	10.02
second vertical bending of car body	27.83
third vertical bending of car body	54.56

In Fig. 8, the RMS values of the vibration acceleration of the vehicle car body using the H_∞ optimal controller and passive suspension vehicle are compared at different operating speeds. It can be observed that the RMS value of the vibration acceleration of the combined control vehicle is smaller than that of the passive suspension. The greater the speed, the better is the vibration acceleration suppression effect. The vibration acceleration decreased by 0.004 m·s^{-2} at 200 km·h^{-1}, which is a reduction of 10%, and the vibration acceleration decreased by 0.018 m·s^{-2} at 350 km·h^{-1}, which is a reduction of 18%.

Fig. 9 shows the force PSDs of the secondary actuator. It can be seen that the PSDs of the output force of the

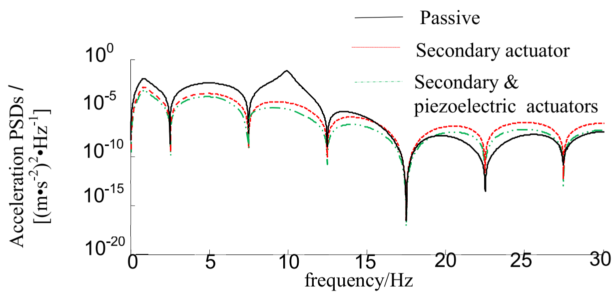

FIGURE 6. Acceleration PSDs on car body center.

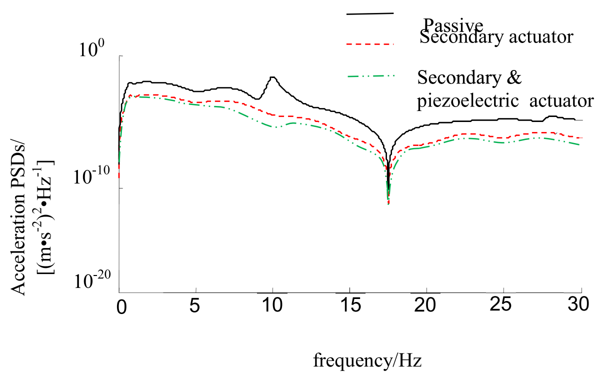

FIGURE 7. Acceleration PSDs above bogie.

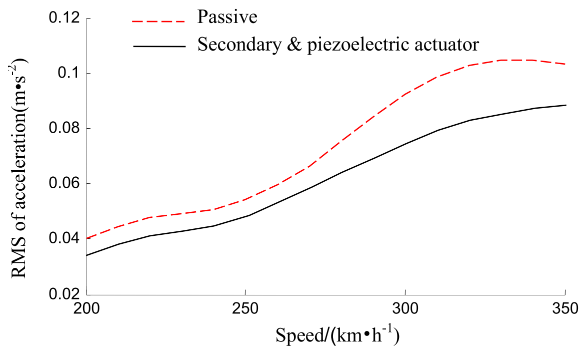

FIGURE 8. Curves of acceleration and speed on car body center.

secondary actuator are 10^{6}N^2·Hz^{-1} at the bounce and pitch vibration frequencies of the car body. This shows that the output force of the secondary vertical actuator is large in this frequency band, which significantly inhibits the rigid vibration of the vehicle car body. The PSDs of the output force of the secondary actuator was 10^{3}N^2·Hz^{-1} at the second vertical bending frequency. This shows that the output force was small at this frequency, and the vibration suppression effect on the vehicle car body was small.

Fig. 10 shows the output voltage PSDs of the piezoelectric actuator. It can be seen that the piezoelectric actuator output voltage PSDs are large in the frequency range of 0–15 Hz, particularly at the first vertical bending vibration frequency of the vehicle car body. The voltage PSDs reached a peak value of 4000 V^2·Hz^{-1}, indicating that the first vertical bending

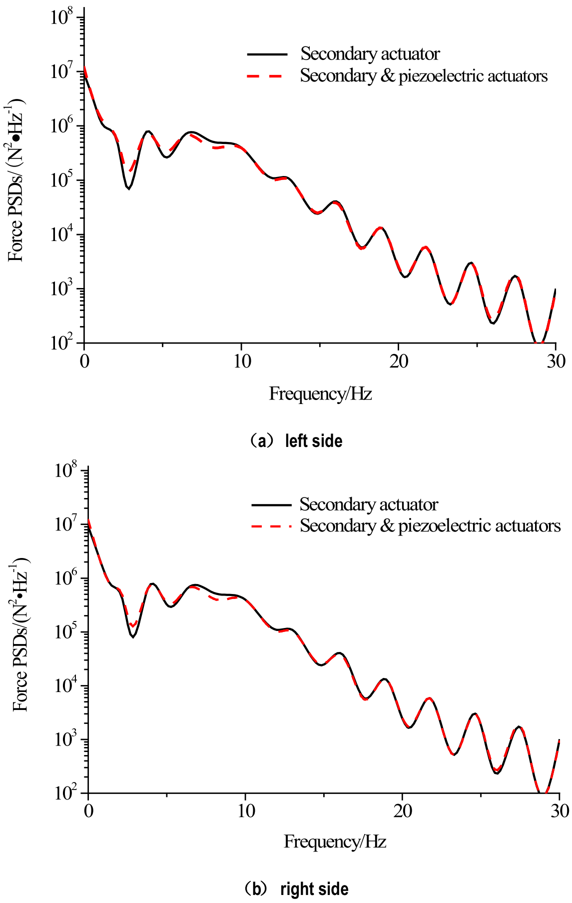

FIGURE 9. Secondary vertical actuator force PSDs.

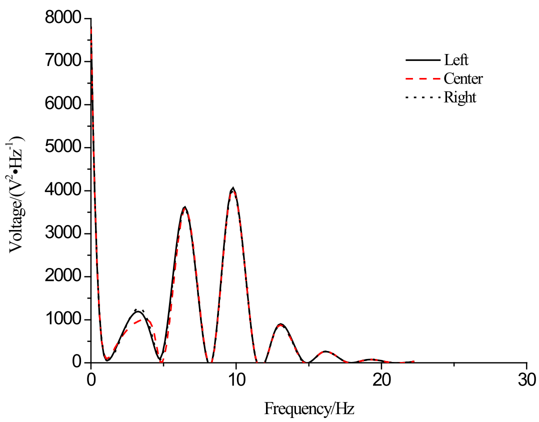

FIGURE 10. Piezoelectric actuator voltage PSDs.

elastic vibration of the vehicle car body was effectively controlled by the piezoelectric actuator.

VI. CONCLUSION

(1) According to the principle of vibration reduction, an EMU vehicle vibration reduction method is proposed, in which the electro-hydraulic actuator is installed at the secondary suspension and the piezoelectric actuator is mounted on the side frame of the car body. The vehicle system mechanics model of vibration reduction was designed with an active suspension H_∞ optimal controller. The analysis results show that the method can significantly reduce the rigid and elastic vibrations of the car body, particularly the first vertical bending vibration of the car body. The greater the speed, the better is the vibration acceleration suppression effect.

(2) The piezoelectric actuator and sensor position arrangement can be optimized by normalizing H_2/H_∞ norm. To avoid the overflow problem caused by modal truncation, piezoelectric actuators and sensors should adopt collocation control.

(3) The simulation results show that the control voltage of the piezoelectric actuators and the output force of the electro-hydraulic actuators can satisfy the control requirements when the H_∞ robust optimal control is adopted. It can suppress the vibration of the vehicle car body and improve the ride comfort.

We have presented a robust optimal control method based on secondary vertical actuators and piezoelectric actuators which can effectively suppress the vibration of the railway car body. The acceleration power spectrums of the first order vertical bending vibration frequency on car body center and above bogie are reduced to 5% and 10% of passive suspension vehicle respectively. The greater speed, the better vibration acceleration suppression effect is obvious. The effectiveness of this method for vehicle body vibration reduction is analyzed by simulation, which can apply to vehicle structure design. However, due to the limitations of simulation, the proportional test bench and vehicle test research should be carried out. Furthermore, how to apply the proposed method to complicated nonlinear systems is the direction of research in the future.

REFERENCES

[1] H. Shi and P. Wu, "Flexible vibration analysis for car body of high-speed EMU," *J. Mech. Sci. Technol.*, vol. 30, pp. 55–66, Jan. 2016.

[2] L. Ling, Q. Zhang, X. Xiao, Z. Wen, and X. Jin, "Integration of car-body flexibility into train–track coupling system dynamics analysis," *Vehicle Syst. Dyn.*, vol. 56, no. 4, pp. 485–505, Apr. 2018.

[3] G. Diana, F. Cheli, A. Collina, R. Corradi, and S. Melzi, "The development of a numerical model for railway vehicles comfort assessment through comparison with experimental measurements," *Vehicle Syst. Dyn.*, vol. 38, no. 3, pp. 165–183, Sep. 2002.

[4] C. H. Huang and J. Zeng, "Flexural vibration suppression of car body for high-speed passenger car based on constrained damping layers," *J. Traffic Transp. Eng.*, vol. 10, no. 1, pp. 36–42, Jan. 2010.

[5] M. Kozek, C. Benatzky, A. Schirrer, and A. Stribersky, "Vibration damping of a flexible car body structure using piezo-stack actuators," *Control Eng. Pract.*, vol. 19, no. 3, pp. 298–310, Mar. 2011.

[6] E. Foo and R. M. Goodall, "Active suspension control of flexible-bodied railway vehicles using electro-hydraulic and electro-magnetic actuators," *Control Eng. Pract.*, vol. 8, no. 5, pp. 507–518, May 2000.

[7] Y. Sugahara, A. Kazato, R. Koganei, M. Sampei, and S. Nakaura, "Suppression of vertical bending and rigid-body-mode vibration in railway vehicle car body by primary and secondary suspension control: Results of simulations and running tests using shinkansen vehicle," *Proc. Inst. Mech. Eng. F, J. Rail Rapid Transit*, vol. 223, no. 6, pp. 517–531, Nov. 2009.

[8] H. Cao, W. H. Zhang, and B. R. Miao, "Vertical vibration analysis of the flexible carbody of high speed train," *Int. J. Veh. Struct. Syst.*, vol. 7, no. 2, pp. 55–60, Feb. 2015.

[9] S. O. R. Moheimani, "A survey of recent innovations in vibration damping and control using shunted piezoelectric transducers," *IEEE Trans. Control Syst. Technol.*, vol. 11, no. 4, pp. 482–494, Jul. 2003.

[10] T. Kamada, K. Hiraizumi, and M. Nagai, "Active vibration suppression of lightweight railway vehicle body by combined use of piezoelectric actuators and linear actuators," *Vehicle Syst. Dyn.*, vol. 48, no. 1, pp. 73–87, Dec. 2010.

[11] S. Leleu, H. Abou-Kandil, and Y. Bonnassieux, "Piezoelectric actuators and sensors location for active control of flexible structures," *IEEE Trans. Nucl. Sci.*, vol. 50, no. 6, pp. 1577–1582, Jun. 2001.

[12] W. Gawronski, *Advanced Structural Dynamics and Active Control of Structures*. New York, NY, USA: Springer, 2004, pp. 167–180.

[13] C. Benatzky and M. Kozek, "Influence of actuator size and location on robust stability of actively controlled flexible beams," in *Proc. 17th World Congr. IFAC*, Seoul, South Korea, 2008, pp. 11859–11864.

[14] D. Halim and S. O. R. Moheimani, "Spatial resonant control of flexible structures-application to a piezoelectric laminate beam," *IEEE Trans. Control Syst. Technol.*, vol. 9, no. 1, pp. 37–53, Jan. 2001.

[15] X. Zheng, A. Zolotas, and R. Goodall, "Combined active suspension and structural damping control for suppression of flexible bodied railway vehicle vibration," *Vehicle Syst. Dyn.*, vol. 58, no. 2, pp. 198–228, Feb. 2019.

[16] D. Halim and S. O. R. Moheimani, "Spatial H_2 control of a piezoelectric laminate beam: Experimental implementation," *IEEE Trans. Control Syst. Technol.*, vol. 10, no. 4, pp. 533–546, Jul. 2002.

[17] A. Orvnäs, S. Stichel, and R. Persson, "Active lateral secondary suspension with H_∞ control to improve ride comfort: Simulations on a full-scale model," *Vehicle Syst. Dyn.*, vol. 49, no. 9, pp. 1409–1422, Sep. 2011.

[18] S. M. M. Bideleh, T. X. Mei, and V. Berbyuk, "Robust control and actuator dynamics compensation for railway vehicles," *Vehicle Syst. Dyn.*, vol. 54, no. 12, pp. 1762–1784, Dec. 2016.

[19] C. H. Huang, J. Zeng, P.-B. Wu, and R. Luo, "Study on car body flexible vibration reduction for railway passenger carriage," *Eng. Mech.*, vol. 27, no. 10, pp. 250–256, Oct. 2010.

HUI CAO received the Ph.D. degree in vehicle engineering from Southwest Jiaotong University, Chengdu, China, in 2016. He is currently an Associate Professor with the College of Intelligent Manufacturing, Chengdu Technological University. He has authored more than 20 articles. His research interests include mechanical optimization design, modeling, and dynamics of vehicle systems.

GANGJUN LI received the Ph.D. degree in vehicle engineering from Southwest Jiaotong University, Chengdu, China, in 2001. He is currently a Professor with the College of Intelligent Manufacturing, Chengdu Technological University. His research interests include optimization design, modeling, and dynamics of robot systems.

NING LIANG received the M.S. degree in management from Chang'an University, Xi'an, China, in 2007. She is currently an Associate Professor with the Sichuan Technology and Business College. Her research interests include marketing and management.